

# Structural and magnetic properties of the alternating Heisenberg spin-chain compound dichloro(2,5-dithiahexane)copper(II)

E. Herrling, G. Fischer, S. Matejcek, and B. Pilawa  
*Physikalisches Institut, Universität Karlsruhe (TH), 76128 Karlsruhe, Germany*

H. Henke  
*Institut für Anorganische Chemie, Universität Karlsruhe (TH), 76128 Karlsruhe, Germany*

I. Odenwald and W. Wendl  
*Kristall- und Materiallabor, Universität Karlsruhe (TH), 76128 Karlsruhe, Germany*  
 (Received 27 June 2002; published 16 January 2003)

Temperature dependence and anisotropy of the electron-spin-resonance (ESR) signal at 9.5 GHz of the one-dimensional alternating Heisenberg antiferromagnet dichloro(2,5-dithiahexane)copper(II) are reported in the temperature range between 5 and 300 K. The ESR measurements reveal a structural phase transition at  $T_c \approx 150$  K. By x-ray diffraction the structure of the low-temperature phase is determined at  $T = 120$  K. Symmetry reduction from the monoclinic space group  $P2_1/n$  to the triclinic group  $P\bar{1}$  results in the formation of twin domains and the creation of two different kinds of spin chains below  $T_c$ . The influence of the structural modifications on the magnetic properties is discussed in detail. Measurements of the static magnetic susceptibility yield the exchange constants and alternation parameters  $J_1/k_B = -29.3(1)$  K,  $\alpha_1 = 0.76(1)$  and  $J_2/k_B = -27.9(1)$  K,  $\alpha_2 = 0.99(1)$  of chain 1 and 2, respectively.

DOI: 10.1103/PhysRevB.67.014407

PACS number(s): 61.10.Nz, 76.30.-v, 75.20.Ck

## I. INTRODUCTION

The alternating Heisenberg spin-1/2 chain is one of the simplest nontrivial quantum systems and there are many substances whose magnetic properties are well approximated by the spin Hamiltonian

$$\mathcal{H}(J, \alpha) = -J \sum_i (\vec{s}_{2i} \vec{s}_{2i-1} + \alpha \vec{s}_{2i} \vec{s}_{2i+1}), \quad (1)$$

$$\text{or } \mathcal{H}(J^*, \delta) = -J^* \sum_i [1 - (-1)^i \delta] \vec{s}_i \vec{s}_{i+1},$$

with the exchange constant  $J^* = J(1 + \alpha)/2$  and the alternation parameters  $\delta = (1 - \alpha)/(1 + \alpha)$ .<sup>1-3</sup> Both notations of the spin Hamiltonian are frequently used in the literature.

The basic difference between the uniform ( $\delta = 0$ ) and alternating spin chain ( $\delta \neq 0$ ) consists in the energy gap which separates the ground state from the first excited states. For the uniform chain there is no gap whereas for the extremely dimerized chain ( $\alpha = 0$ ) the smallest excitation energy is  $\Delta = |J|$ . The early experiments on the triplet excitons observed in organic compounds stimulated the theoretical interest in the spin gap and the dispersion of the  $S = 1$  excited state.<sup>4</sup> Solutions of Hamiltonian (1) were presented by Bulaevskii in terms of a Hartree-Fock scheme,<sup>5</sup> by low-temperature perturbation calculation<sup>6</sup> and renormalization-group theory which predicts that for  $\delta \rightarrow 0$  the spin gap should close according to  $\Delta \propto \delta^{2/3}/|\ln \delta|^{1/2}$ .<sup>7-9</sup>

One important reason for the renewed interest in alternating spin chains results from the prediction of quantum-field theory that the antiferromagnetic alternating Heisenberg spin-1/2 chain and uniform spin-1 Heisenberg antiferromag-

netic chain belong to the same universality class of quasi-one-dimensional magnets as the spin-ladder systems with an even number of coupled spin chains.<sup>10-12</sup> Indeed, the phase diagrams of these systems have the same structure. At low temperatures when the dynamic properties are dominated by quantum fluctuations there are two critical magnetic fields. The first critical field  $H_{c1}$  separates the gapped spin liquid phase from the gapless incommensurate phase between  $H_{c1}$  and  $H_{c2}$ . At the second critical field  $H_{c2}$ , the system enters the fully aligned ferro-type phase.

For some time the vanadates  $\text{NaV}_2\text{O}_5$  and  $(\text{VO})_2\text{P}_2\text{O}_7$  were considered as possible spin-ladder compounds<sup>13</sup> but later characterized by the alternating chain Hamiltonian.<sup>14,9,15</sup> Due to the high exchange couplings  $|J|/k_B \approx 116$  K [ $(\text{VO})_2\text{P}_2\text{O}_7$ ] and  $|J|/k_B \approx 464$  K ( $\text{NaV}_2\text{O}_5$ ) the accuracy of the old theoretical calculations on alternating spin chains<sup>16-19</sup> had to be improved for the analysis of these compounds. This was done by Augier *et al.*,<sup>20</sup> Barnes *et al.*,<sup>21</sup> and Konstantinovic *et al.*<sup>22</sup> who showed that the spin gap can be approximated extremely well by the simple formula  $\Delta = 2J^* \delta^{3/4}$ . Johnston *et al.*<sup>9</sup> pointed out that the deviation of the exponent from 3/4 is smaller than 2% and the critical regime where logarithmic corrections become important is expected below  $\delta \approx 0.005$  ( $\alpha > 0.99$ ).

Due to the comparatively large exchange constants of purely inorganic compounds the investigation of metal-organic substances presents an attractive alternative approach as is demonstrated by the work on the spin-ladder substance  $\text{Cu}_2(\text{C}_5\text{H}_{12}\text{N}_2)_2\text{Cl}_4$  (Ref. 11) and the alternating spin chain compound  $\text{Cu}(\text{NO}_3)_2 \cdot 2.5\text{H}_2\text{O}$  which is characterized by  $J/k_B = -5.2$  K and  $\alpha = 0.27$ .<sup>23</sup> The thermodynamic properties were measured over the whole interesting field range below  $H_{c1}$ , between  $H_{c1}$  and  $H_{c2}$ , and above  $H_{c2}$  and com-

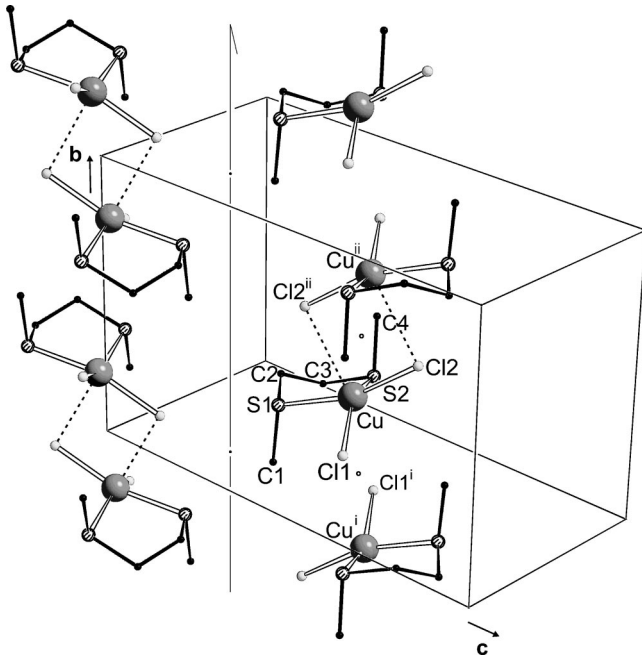


FIG. 1. Unit cell of Cu-DTH at room temperature showing the position of a  $2_1$  screw axis and of two centers of inversion as small circles. Dotted lines indicate dimer formation. The infinite “copper chain”  $\cdots\text{Cu}^i, \text{Cu}, \text{Cu}^{ii}\cdots$  extending in **b** direction is repeated by virtue of the screw axis on the left. The symmetry code is defined in Sec. III B.

pared with theoretical predictions based on numerical diagonalization of finite spin systems.<sup>24</sup> Diederix *et al.*<sup>25–28</sup> studied in detail the spin dynamics of the alternating spin chain by  $^1\text{H}$  nuclear magnetic resonance. Considering the current interest in quantum critical phenomena and quantum liquids this work is still of high relevance and the studies of  $\text{Cu}(\text{NO}_3)_2 \cdot 2.5\text{D}_2\text{O}$  by neutron scattering are just at the beginning.<sup>29</sup>

In this paper, we investigate the alternating spin chain compound dichloro(2,5-dithiahexane)Cu(II) (Cu-DTH). This substance was synthesized by Hatfield *et al.*<sup>30</sup> Figure 1 shows the monoclinic unit cell at room temperature as reported by Hatfield *et al.*<sup>30</sup> (space group  $P2_1/n$ ,

$a=6.875 \text{ \AA}$ ,  $b=8.963 \text{ \AA}$ ,  $c=14.513 \text{ \AA}$ ,  $\beta=90.48^\circ$ ). The  $\text{Cu}^{II}$  ion is coordinated by two chlorine and two sulfur atoms. The coordination of the Cu ion is not planar (see Table I) and the complexes form stacks of centrosymmetric dimers with short  $\text{Cu}\cdots\text{Cl}(2)$  contacts of the length  $3.074 \text{ \AA}$  (dotted lines in Fig. 1). This gives rise to the formation of infinite alternating chains along **b**. The Cu-DTH complexes within the unit cell are related by the  $2_1$  screw operation which leads to two *magnetically* inequivalent chains already at room temperature. The magnetic properties were determined by measurements of the static magnetic susceptibility. Due to an anomaly at 26 K and the fact that the crystals shatter upon cooling, Hatfield *et al.*<sup>30</sup> concluded that there is a structural phase transition and the resulting phase was characterized by an exchange constant of  $J/k_B = -28.8 \text{ K}$  and the alternation parameter  $\alpha=0.87$ .

The plan of the paper is as follows. The results of the ESR measurements are summarized in Sec. II. These measurements reveal a structural phase transition at  $T_c \approx 150 \text{ K}$  resulting in a specific domain structure. No further anomaly could be detected especially around  $\sim 26 \text{ K}$  as observed by Hatfield *et al.*<sup>30</sup> Measurements of the ESR, the static magnetic susceptibility and the heat capacity confirm that there is no additional phase transition down to  $\sim 5 \text{ K}$ . The crystal structure of Cu-DTH is discussed in Sec. III. X-ray diffraction shows that the two-fold screw axis is lost during the phase transition which leads to the formation of two *crystallographically* inequivalent chains. These results are needed for the discussion of the ESR measurements in Sec. IV. Based on these results the magnetic susceptibility is analyzed in Sec. V leading to values of the exchange constants and alternation parameters.

## II. ESR MEASUREMENTS

The Cu-DTH complexes were synthesized according to Hatfield *et al.*<sup>30</sup> The crystals form dark green nearly rectangular plates ( $1 \text{ mm} \times 0.3 \text{ mm} \times 0.02 \text{ mm}$ ) with the crystallographic **b** direction parallel to the long side of the plates and the **c** direction normal to the plates. On air the crystals degrade presumably due to humidity since the coordinating

TABLE I. Some structural parameters of Cu-DTH above and below the phase transition.

	$T=300 \text{ K}$	$T=120 \text{ K}$ (chain 1)	$T=120 \text{ K}$ (chain 2)
$\angle(\text{Cl-Cu-Cl}; \text{S-Cu-S})^a$	$37.16^\circ$	$37.31^\circ$	$35.29^\circ$
$\angle(\text{S-Cu-S}; \mathbf{b})^b$	$17.87^\circ$	$17.73^\circ$	$10.92^\circ$
$\angle(\text{Cu}\cdots\text{Cu}; \text{S-C})_{\text{intra}}^c$	$24.17^\circ$	$29.44^\circ$	$18.79^\circ$
$\text{Cu}\cdots\text{Cu}$ (intradimer)	$3.948 \text{ \AA}$	$3.817 \text{ \AA}$	$4.117 \text{ \AA}$
$\angle(\text{Cu}\cdots\text{Cu}; \text{S-C})_{\text{inter}}$	$7.28^\circ$	$9.64^\circ$	$11.51^\circ$
$\text{Cu}\cdots\text{Cu}$ (interdimer)	$5.058 \text{ \AA}$	$4.956 \text{ \AA}$	$4.647 \text{ \AA}$
$\text{S}\cdots\text{S}^d$	$3.856 \text{ \AA}$	$3.629 \text{ \AA}$	$3.686 \text{ \AA}$

<sup>a</sup>angle between the normal of the Cl-Cu-Cl plane and the S-Cu-S plane.

<sup>b</sup>angle between the normal of the S-Cu-S plane and **b**. The angle between the S-Cu-S planes of chain 1 and chain 2 is  $8.34^\circ$ .

<sup>c</sup>angle between the vector connecting the Cu ions and the S-CH<sub>3</sub> bond axis.

<sup>d</sup> $\text{S}(1)\cdots\text{S}(2^{iv})$  and  $\text{S}(3)\cdots\text{S}(4^{iv})$  for chain 1 and 2, respectively, denote the shortest interchain contacts.

DTH ligand can be replaced by water molecules. This effect leads to a defect signal which is visible in the ESR spectra (Figs. 5 and 7). In the dry atmosphere of an exsiccator the crystals are stable.

ESR was measured with a Bruker ESP300E X-band spectrometer equipped with a rectangular cavity and an Oxford ESR900 cryostat. During the measurements the sample was covered by vacuum grease which protects the crystal sufficiently.

Figure 2 shows the temperature dependence of the ESR linewidth  $\Delta B_{1/2}$  (half-width at half-maximum) when the magnetic field is applied along **a** and **b**, respectively.

$\Delta B_{1/2}$  decreases linearly upon cooling down from room temperature. At 144 K there is a jump which is followed by a temperature range, where  $\Delta B_{1/2}$  is nearly constant. Below 100 K  $\Delta B_{1/2}$  increases up to a maximum at about 20 K and drops to small values at lower temperatures. When the crystal is heated from low temperatures the jump of  $\Delta B_{1/2}$  occurs at 156 K. This hysteresis is a clear sign for a first-order structural phase transition. The size of the jumps of  $\Delta B_{1/2}$  depends on the sweeping rate and the start temperature. This indicates relaxation times of the structural transformation in the range of hours. The open symbols in Fig. 2 show a temperature sweep just around  $T_c$ .

Figure 3 displays the temperature dependence of the  $g$  factor. Above the transition temperature  $g$  shifts smoothly with temperature which indicates a temperature-dependent reorientation of the Cu-DTH complexes. The enhanced spin-lattice relaxation due to this effect is also reflected in the linear increase of  $\Delta B_{1/2}$  with increasing temperature. The phase transition leads to a jump and a hysteresis of  $g$ . Below the transition temperature,  $g$  is essentially constant which indicates the stability of the new crystal structure. The small temperature dependence below  $\sim 50$  K reflects an internal magnetic field due to static correlations of the magnetic moments.

Below the transition temperature the ESR line splits for special orientations of the magnetic field into two components which indicates the formation of a two-domain structure.

The modification of the anisotropy of  $\Delta B_{1/2}$  and the  $g$  factor due to the phase transition are shown in Fig. 4 which displays the angular variation of  $g$  and  $\Delta B_{1/2}$  in three orthogonal planes for temperatures above and below the phase

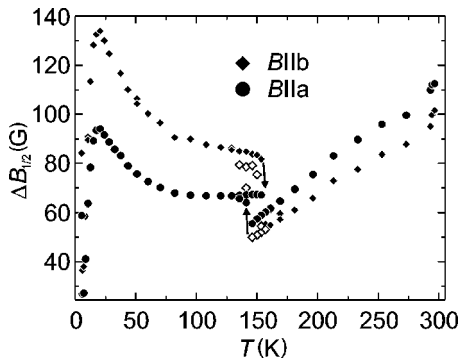


FIG. 2. Temperature dependence of  $\Delta B_{1/2}$ . The open symbols show a temperature sweep just around  $T_c$ .

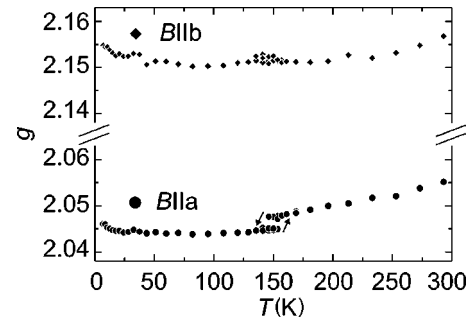


FIG. 3. Temperature dependence of the  $g$  factor.

transition. Here **a**, **b**, and **c** correspond to the nearly orthogonal directions of the lattice base vectors of the high-temperature phase.

Below the transition temperature two separate lines can be resolved in the **b-c** plane. An example is shown in Fig. 5. The derived maxima and minima of  $g$  of the two domains below the transition temperature shift about  $\pm 10^\circ$  with respect to **b**. In the **a-c** plane, there is always one Lorentzian resonance line and no line splitting can be detected. In the **a-b** plane there is only a tiny splitting which can be resolved for temperatures below 20 K when  $\Delta B_{1/2}$  becomes small. The corresponding angular variation of  $\Delta B_{1/2}$  and the  $g$  factor is shown in Fig. 6. The maxima and minima of  $g$  of the **a-b** plane are shifted by  $\sim \pm 3.5^\circ$ . Especially around  $170^\circ$  it is difficult to separate accurately the two lines. Figure 7 gives an example for the analysis of this tiny line splitting.

### III. X-RAY DIFFRACTION

#### A. Experimental

X-ray powder data were recorded by means of a STOE StadiP diffractometer equipped with a helium closed-cycle refrigerator system. The sample was sealed in a glass capillary with some silicon added for calibration. Using Gemonochromated copper radiation ( $\lambda = 1.540562 \text{ \AA}$ ) the refinement of the cell parameters was performed with the angular positions obtained by profile fits of 28 powder lines.

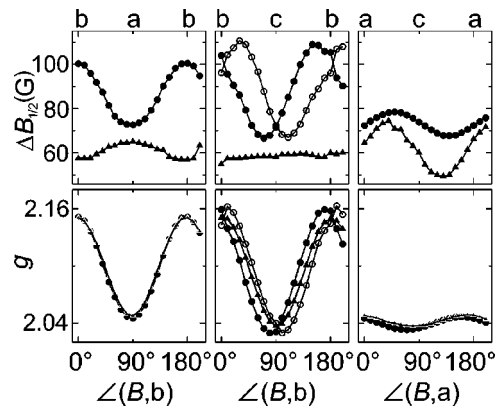


FIG. 4. Anisotropy of the  $g$  factor and  $\Delta B_{1/2}$  in three orthogonal planes. Triangles for  $T = 169$  K, full and open circles for  $T = 60$  K. The full and open circles distinguish between the signal of the two kinds of domains.

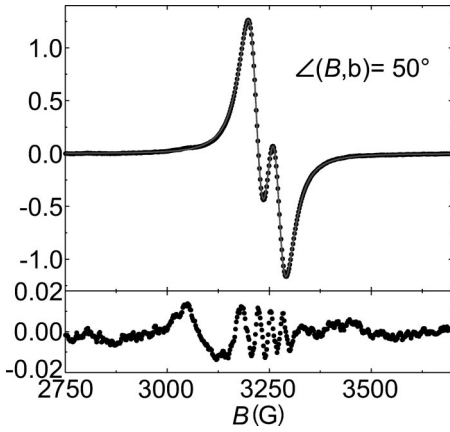


FIG. 5. Dots, ESR signal in the **b-c** plane at  $T=6$  K, solid line, fit of two Lorentzian lines. The lower curve shows the difference between the experimental data and the fit of two Lorentzian ESR lines. There is a small defect signal in the left wing of the resonance (see also Fig. 7).

For single-crystal work a specimen of Cu-DTH was cut to the dimensions of  $0.2 \times 0.25 \times 0.04$  mm<sup>3</sup> (from a still longer needle-shaped platelet) and sealed in a glass capillary. The measurements were carried out on a STOE four-circle diffractometer with specialized control software to ensure the collection of as many overlap-free reflection intensities as possible in the case of a nonmerohedral twin. For reflections with overlapping twin components the common intensity of both twin individuals was measured as long as their scattering vectors could be oriented horizontally.<sup>31</sup>

Cooling of the sample to 120 K was achieved with a stream of cold nitrogen gas ( $\Delta T = \pm 2$  K, equipment Nicolet LT-1, temperature calibration by KDP). Severe resolution problems arose from the fact that below  $T_c$  the crystal splits up into lamellas slightly canted against each other so that the effective broadness of the reflection profiles was increased to at least  $1.2^\circ$  ( $\omega$ ). This complicated the search for the twin law and integrations over the fractured profiles.

The compromise between not cutting-off intensity and resolving individual peaks well enough led to unsatisfactory results in quite a number of instances, a fact which is also reflected in rather high values of the residuals (see below),

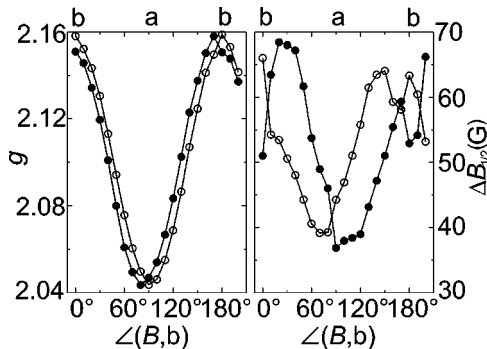


FIG. 6. Anisotropy of the  $g$  factor and  $\Delta B_{1/2}$  in the **a-b** plane at  $T=8.5$  K. The full and open circles distinguish between the signals of the two kinds of domains.

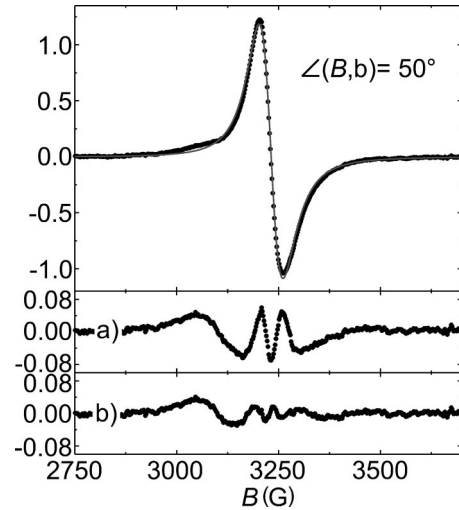


FIG. 7. Dots, ESR signal in the **a-b** plane at  $T=8.5$  K, solid line, fit with one Lorentzian line. The lower curves show the difference between the experimental data and the fit of one (a) and two Lorentzian ESR lines (b). At  $\sim 3050$  G a small defect signal is found.

but the structure could be solved starting from two very small atomic fragments. The latter were expanded step by step by the cyclic use of refinements and difference Fourier syntheses with the program SHELX97 (Sheldrick, 1997).<sup>32</sup> The final refinement included anisotropic displacement parameters for the atom types Cu, Cl, and S. All hydrogen positions were calculated (routine HFIX of SHELXL97, loc cit).<sup>32,48</sup>

From 2255 reflections successfully measured, 425 were resolved, 1830 consisted of overlapping pairs with the common intensity obtained by a  $\psi$  scan, the rest of 1871 reflections was not accessible due to orientational problems (angle restrictions of the instrument) giving a total of 4126 measurements attempted up to a limit of  $2\theta_{max} = 55^\circ$ . The final residuals were  $wR_2 = 0.174$  for all data and 127 structure parameters,  $R_1 = 0.061$  for  $1764 F_o > 4\sigma F_o$ , residual electron density  $\Delta\rho_{min/max} = -1.47/1.25 e/\text{\AA}^3$ .

### B. Results from x-ray diffraction

Initially, the powder diagrams of Cu-DTH above and below  $T_c$  were compared to obtain information about the cell-metrical changes ascribed to the phase transition. The powder pattern of the low-temperature form can be indexed on the basis of a triclinic cell with  $a = 6.772(2)$ ,  $b = 8.722(3)$ ,  $c = 14.852(7)$  \AA,  $\alpha = 93.45(2)$ ,  $\beta = 93.66(2)$ ,  $\gamma = 90.19(2)^\circ$  at 120 K. Later on it seemed appropriate to modify this cell setting in order to aid the comparison with the monoclinic high-temperature phase. The necessary transformation is as follows:  $\mathbf{a}' = \mathbf{a}$ ,  $\mathbf{b}' = -\mathbf{b}$ ,  $\mathbf{c}' = -\mathbf{c}$  with  $\beta' = 180^\circ - \beta$ , and  $\gamma' = 180^\circ - \gamma$ . This leads to the unconventional final setting used for the description of the triclinic modification of Cu-DTH and the atomic coordinates from the structure refinement with SHELXL97 (loc cit) given in Table II.<sup>32,48</sup>

Table I contains a selection of characteristic structural parameters and Fig. 8 shows the unit cell at 120 K. The sym-

TABLE II. Atomic coordinates for Cu-DTH at 120 K referred to the actual unit cell with  $a' = 6.772(2)$ ,  $b' = 8.722(3)$ ,  $c' = 14.852(7)$  Å and  $\alpha' = 93.45(2)$ ,  $\beta' = 86.34(2)$ ,  $\gamma' = 89.81(2)^\circ$ .

Atom	$x$	$y$	$z$
Cu(1)	0.5329	0.2164	0.4935
Cl(1)	0.2867	0.0898	0.5640
Cl(2)	0.6567	0.3339	0.6176
S(1)	0.3462	0.2483	0.3690
S(2)	0.8123	0.2743	0.4083
C(1)	0.2744	0.0555	0.3313
C(2)	0.5277	0.2931	0.2809
C(3)	0.7329	0.2275	0.2972
C(4)	0.8335	0.4837	0.4118
Cu(2)	-0.0115	0.2334	-0.0133
Cl(3)	-0.2682	0.3450	0.0660
Cl(4)	0.1211	0.1131	0.0982
S(3)	-0.1654	0.2630	-0.1459
S(4)	0.2967	0.2509	-0.0903
C(5)	-0.1966	0.4712	-0.1509
C(6)	0.0373	0.2259	-0.2286
C(7)	0.2271	0.2994	-0.2013
C(8)	0.3718	0.0536	-0.1121

metry code applying throughout in this paper is as follows: (i)  $1-x, -y, 1-z$ , (ii)  $1-x, 1-y, 1-z$ , (iii)  $-x, -y, -z$ , (iv)  $x-1, y, z$ . The observed symmetry change from  $P2_1/n$  to  $P\bar{1}$  accounts for the formation of twin domains which have the axis  $[010]$  in common, thus, giving a twofold rotation twin. Obviously, the existence of a simple group-subgroup relation<sup>33</sup> of type t2 does not prevent the transition

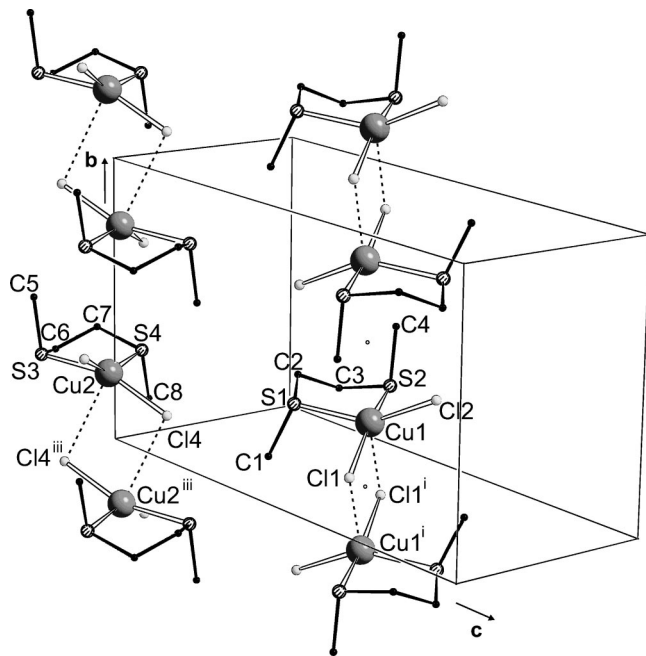
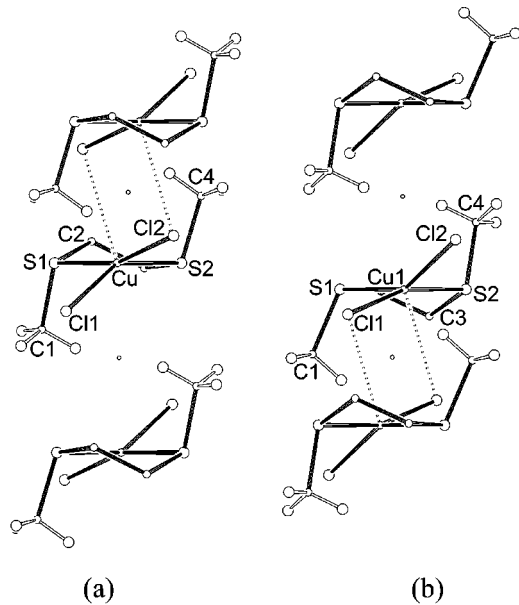


FIG. 8. Unit cell of Cu-DTH at 120 K. Dotted lines around the centers of inversion (small circles) mark the dimerization sites.



$$\begin{aligned} \angle(\text{S}(1)\text{-C}(2)\text{-C}(3)\text{-S}(2)) &= -53.1^\circ & \angle(\text{S}(1)\text{-C}(2)\text{-C}(3)\text{-S}(2)) &= -51.0^\circ \\ \angle(\text{C}(2)\text{-C}(3)\text{-S}(2)\text{-Cu}) &= 32.4^\circ & \angle(\text{Cu}(1)\text{-S}(1)\text{-C}(2)\text{-C}(3)) &= 25.7^\circ \\ \angle(\text{C}(3)\text{-S}(2)\text{-Cu-S}(1)) &= -4.3^\circ & \angle(\text{S}(2)\text{-Cu}(1)\text{-S}(1)\text{-C}(2)) &= 1.5^\circ \\ \angle(\text{S}(2)\text{-Cu-S}(1)\text{-C}(2)) &= -18.3^\circ & \angle(\text{C}(3)\text{-S}(2)\text{-Cu}(1)\text{-S}(1)) &= -22.9^\circ \\ \angle(\text{Cu-S}(1)\text{-C}(2)\text{-C}(3)) &= 44.0^\circ & \angle(\text{C}(2)\text{-C}(3)\text{-S}(2)\text{-Cu}(1)) &= 47.5^\circ \end{aligned}$$

FIG. 9. Comparison of corresponding segments in (a) the high-temperature form and (b) the low-temperature form of Cu-DTH for chain 1. The conformational change by *pseudorotation* as quantified by the torsional angles results in a shift of the dimer formation from the upper to the lower part of the figure (see dotted lines, further details are given in the text). Vector **b** approximately vertical, centers of inversion given as small circles.

to be typically first order as the metrical changes and the observed hysteresis effects demonstrate clearly.

In space group  $P\bar{1}$  the conformation of the copper complexes and their linkage to pairs of centrosymmetric dimers along **b** is retained, at least in principle. Under the reduced symmetry the chains around Cu(1) and Cu(2), related by a  $2_1$  screw operation above  $T_c$ , are now decoupled. For chain 1 the site where the dimerization takes place moves to the same layer height as in the neighboring chain 2 (see Figs. 8 and 9). This is the main reason why the screw axis is given up. The transformation involves

- (i) a conformational change within the Cu-DTH complex,
- (ii) an interchange between the longer and the shorter Cu...Cu distance,
- (iii) a turn of the bridging plane by nearly  $90^\circ$  since here instead of Cl(2) the dimerization is effected by Cl(1),
- (iv) rotational adaptations for the complex unit around Cu(1).

Chain 2—attributed to atom Cu(2)—compares more directly with its counterpart (not the asymmetric unit) of the high-temperature form. Modifications are merely necessary concerning the tilt of the S-Cu-S plane and the Cu...Cu

distances becoming more equal within the chain such that the interdimer separation is reduced at the expense of the contact distances within the dimer (see Table I).

While the complex around Cu(2) represents an inverted image<sup>34</sup> as compared to the asymmetric unit above  $T_c$ , a direct mapping can be tried for Cu(1) (see Table I). The horizontally aligned S-Cu-S plane (see Fig. 9) serves as internal reference for the five-membered ring which originates from the ligand attached to the copper center. The pattern of torsional angles agrees well with the situation before the phase change (individual differences not larger than  $7^\circ$ ), but only if it is accepted that either Fig. 9(a) or 9(b) has to be rotated by  $180^\circ$  in the direction of view. In reality, this *pseudorotation* is accomplished by the twisting of bond C(2)-C(3) against the rest of the ring such that afterwards atom C(3) sticks out of the ring plane, a rôle that atom C(2) had before. In the transition state, the local *pseudo*-twofold axis should become more symmetrical when passing the *half-chair* conformation ( $C_2$ ).<sup>35</sup>

The reversal between the longer and shorter Cu...Cu distance correlates with the angle between the vector connecting the Cu ions and the orientation of the S-CH<sub>3</sub> unit serving as a spacer between the complexes as long as this angle is close to  $10^\circ$ , whereas dimerization is permitted for larger values (see Table I). This swap of angles increases the length of lattice parameter  $c$  because directing the methyl group of C(1) towards atom Cl(4) requires additional space (see Fig. 8).

Since now atom Cl(1) acquires the rôle of the bridging partner towards a copper center in the next-lying layer, the site of dimerization is changing height and it is turned by approximately  $90^\circ$ , both with respect to **b**. Recalling that the linkage via Cl(4) stays fixed this new scheme gives rise to a criss-cross arrangement of bridging planes between just one pair of layers in contrast to the high-temperature form. This means, all dimers assemble in double layers of this type.

As shown in Fig. 8 and by the corresponding angles of Table I the ring segments S-Cu-S cannot be expected to be accurately lined up with their plane normals in **b** direction due to the ring puckering and interactions between the complex units. But a characteristic change occurs during the phase transition. In space group  $P2_1/n$  these tilts are held in an opposed alignment by virtue of the screw axis, whereas in  $P\bar{1}$  they are pointing more or less into the same direction. For chain 1 this affords a rotation of all complex units approximately around the line S(1)···S(2) by an angle close to the value of Table I just doubled; i.e.  $2 \times 18^\circ$ . In chain 2 this angle is simply reduced from  $18^\circ$  to  $11^\circ$ .

Still another rotation acts on the complex units of chain 1 (ca.  $3^\circ$  around **b** as estimated from the [010] projection). This smaller rotation in combination with the contraction of lattice parameter  $a$  and the triclinic distortion within the **a-c** plane (angle  $\beta$ ) is made responsible for the decreased length of the interchain contact S(1)···S(2<sup>iv</sup>) between type-1 chains (see Table I). Similarly, the shortening of contact S(3)···S(4<sup>iv</sup>) is explained except that an additional rotation is not observed for chain 2.

Taking into account that during a first-order phase transition normally considerable tensions build up in a crystal (cf.

the metrical changes of the lattice parameters), it seems plausible that the release of these tensions causes the crystal to split up into lamellas.

These observations shed some light on the mechanism which leads to the structural phase transition. From the ESR results it is known that the orientation of the Cu-DTH complexes changes smoothly upon cooling. This opens the possibility to optimize the orientation of the methyl groups at the end of the 2,5-dithiahexane ligand which leads to the phase transition at 150 K. These results contrast with the related compounds dichloro(4,7-dithiadecane)copper(II)<sup>30</sup> and dichloro(3,6-dithiaoctane)copper(II)<sup>36</sup> (Cu-DTO) which show no structural phase transition although the ESR results reveal a comparable reorientation of the Cu-DTO complexes. The substitution of the methyl group by more bulky alkyl groups obviously prevents the structure from running into a phase change.

## IV. DISCUSSION OF THE ESR RESULTS

### A. The $g$ tensor

The principal  $g$  values of a Cu-DTH single crystal at room temperature are  $g = 2.151(1)$  along **b** and  $2.049(1)$ ,  $2.038(1)$  within the **a-c** plane. Due to the inversion symmetry the  $g$  tensors of the Cu-DTH complexes along the chains are equal. The  $g$  tensors of chain 1 and 2 are related by a  $2_1$  screw axis above  $T_c$ . As a consequence of the small but not negligible interchain exchange interaction the ESR signals of chain 1 and 2 are averaged so that the measured  $g$  factor results from the average of  $g$  tensor 1 and 2. The anisotropy of  $g$  above the phase transition in Fig. 4 displays the symmetry around the twofold screw axis along **b**. It is not possible to extract from these data the relation between the structure of the Cu-DTH complex and the orientation of its  $g$  tensor. Assuming an axial  $g$  tensor of the Cu-DTH complex the anisotropy within the **a-c** plane could be attributed to a canting of the  $g$  tensor with respect to **b**. In such a model the canting angle is  $17.6^\circ$  and the eigenvalues of the  $g$  tensor are  $g_{\parallel} = 2.163(1)$  and  $g_{\perp} = 2.0370(5)$ . However, the geometrical structure of the Cu-DTH complex does not support an axial  $g$  tensor. It is known from our ESR measurements of the related compound Cu-DTO that the axial symmetry of the  $g$  tensor is slightly distorted [ $g_1 = 2.1723(1)$ ,  $g_2 = 2.0335(1)$ ,  $g_3 = 2.0296(1)$  at  $T = 200$  K]. Therefore, the small anisotropy recorded in the **a-c** plane reflects the interplay between the orthorhombic distortion and canting of the  $g$  tensors of the Cu-DTH complexes.

The qualitative interpretation of the modifications caused by the structural phase transition has to be based on the assumption that the correlation between the geometry of the Cu-DTH complex and its  $g$  tensor is stable. This seems to be justified since—as it was shown in Sec. III—the geometrical parameters of Cu-DTH complex are only slightly modified by the phase transition (see Table I).

Below the phase transition there are two ESR signals with nearly equal intensity (see Fig. 5) which can be attributed to structural domains. The angular variation of  $g$  below  $T_c$  splits symmetrically with respect to the high-temperature variation in the **a-b** and **b-c** plane but not in the **a-c** plane.

This is reminiscent of the twofold screw axis along  $\mathbf{b}$  which is removed by the phase transition.

The modification of the  $g$  tensors due to the phase transition reflects the structural changes. Above  $T_c$  the small tilts of the  $g$  tensors of chain 1 and 2 with respect to  $\mathbf{b}$  are opposed due to the  $2_1$  screw axis. Consequently the anisotropy of the measured  $g$  factor is symmetric with respect to  $\mathbf{b}$  (Fig. 4). In analogy to the inclination of the (S-Cu-S)-plane discussed above (see Table I), it can be expected that below  $T_c$  the  $g$  tensors of chain 1 and 2 point approximately in the same direction. The averaged ESR signal of chain 1 and 2 is no longer symmetrical with respect to  $\mathbf{b}$  and consequently the  $g$  factors of the domains are shifted with respect to  $\mathbf{b}$ . The effect is strong and easily resolved in the  $\mathbf{b}$ - $\mathbf{c}$  plane (Fig. 4). The shift in the  $\mathbf{a}$ - $\mathbf{b}$  plane is small and can only be resolved for  $T < 20$  K (Fig. 6).

### B. The linewidth

The magnitude and anisotropy of the linewidth  $\Delta B_{1/2}$  is strongly influenced by the structural phase transition. The relation with the structural modifications will be explained in the following. The ESR signals of exchange coupled  $\text{Cu}^{\text{II}}$  ions are mainly broadened by the dipolar interaction and anisotropic components of the exchange interaction between nearest neighbors.<sup>37</sup> Since the smallest distances between Cu ions are realized within the spin chains, the dipolar interaction should lead to a maximum of the linewidth when the magnetic field is applied along  $\mathbf{b}$ . This expectation is not confirmed by the experimental results (compare Fig. 4). Especially above  $T_c$  the maximum of  $\Delta B_{1/2}$  is observed within the  $\mathbf{a}$ - $\mathbf{c}$  plane.

The isotropic exchange interaction is a measure for the strength of the anisotropic exchange interaction.<sup>38–40</sup> As for the dipolar interaction, important contributions can be expected only for the intrachain nearest-neighbor interaction. The antisymmetric Dzyaloshinskii-Moriya interaction is suppressed by the inversion symmetry between the Cu-DTH complexes along the spin chains.<sup>38–40</sup> Therefore, only the pseudodipolar exchange interaction (PD) has to be considered. As in the case of the  $g$  tensor the orientation of the PD tensor is determined by the spin-orbit coupling. In contrast to the  $g$  tensor, the PD-exchange interaction depends on the relative orientation of neighboring complexes.<sup>38–40</sup> This explains why the linewidth is so sensitive to the structural phase transition. It is known that the PD-tensor is frequently similarly oriented as the averaged  $g$  tensor of the interacting copper ions.<sup>41</sup> This simple relation is qualitatively confirmed by the experimental results below  $T_c$  (see Fig. 4). The correlation between the  $g$  factor and the linewidth is visible in the  $\mathbf{a}$ - $\mathbf{b}$  and  $\mathbf{b}$ - $\mathbf{c}$  plane, although the shift of the linewidth maxima in the  $\mathbf{b}$ - $\mathbf{c}$  plane of  $\sim \pm 30^\circ$  with respect to  $\mathbf{b}$  is larger than the corresponding shift of the  $g$  factor ( $\sim \pm 10^\circ$ ) (Fig. 4). These observations indicate that  $\Delta B_{1/2}$  is dominated by the PD-exchange interaction and not by the dipolar interaction.

Below  $T_c$  there are two kinds of domains with two different chains. Due to the structural properties of these chains it can be expected—as for the  $g$ -tensor—that the axes with the

largest main value of the PD tensors for chain 1 and 2 are approximately parallel. This leads for each domain to a large variation of  $\Delta B_{1/2}$  within the  $\mathbf{a}$ - $\mathbf{b}$  and  $\mathbf{b}$ - $\mathbf{c}$  plane.

It is important to note the different orientation of the averaged  $g$  and PD tensors. Although there is only a small tilt of the  $g$  tensor in the  $\mathbf{a}$ - $\mathbf{b}$  plane the shift of the anisotropy of  $\Delta B_{1/2}$  by  $\sim \pm 20^\circ$  with respect to  $\mathbf{b}$  indicates for the PD tensor a large tilt opposite to the direction of the  $g$  tensor (Fig. 6). When the sample is heated above  $T_c$  the anisotropy of  $\Delta B_{1/2}$  in the  $\mathbf{a}$ - $\mathbf{c}$  plane becomes larger whereas the anisotropy of  $\Delta B_{1/2}$  becomes smaller in the other planes (Fig. 4). Since the linewidth variation in the  $\mathbf{a}$ - $\mathbf{c}$  plane reflects the tilt of the PD tensors it can be concluded that this tilt with respect to  $\mathbf{b}$  becomes larger for temperatures above the phase transition. In contrast to the low-temperature phase the PD tensors of chain 1 and 2 are related by the twofold screw axis and hence, oriented in an opposed alignment above  $T_c$ . Consequently, the exchange interaction between chain 1 and 2 leads to an averaged ESR signal with a reduced anisotropy of  $\Delta B_{1/2}$  in the  $\mathbf{a}$ - $\mathbf{b}$  and  $\mathbf{b}$ - $\mathbf{c}$  plane. Based on these ideas it is possible to simulate the experimental results. But it is not possible to determine uniquely the parameters of the intra- and inter-dimer PD-tensor of chain 1 and 2.

Although the structure of Cu-DTH is formed by alternating chains, the ESR results show no typically one-dimensional properties. At high temperatures when the spin dynamics are characterized by diffusion the restriction to one dimension leads to a non-Lorentzian line shape and an enhanced contribution of the secular component of the anisotropic interaction.<sup>42–44</sup>

Instead, the ESR lines are of Lorentzian shape and the anisotropy of  $\Delta B_{1/2}$  is not characterized by an enhancement of the secular components of the anisotropic interactions. The reduction of  $\Delta B_{1/2}$  with decreasing temperature above  $T_c$  as well as the  $g$  shift is, therefore, probably not caused by one-dimensional diffusive spin dynamics but due to spin-lattice relaxation and the reorientation of the Cu-DTH complexes. These results reflect the comparatively soft crystal structure above the phase transition. The increase of  $\Delta B_{1/2}$  for temperatures below  $\sim 70$  K indicates a three-dimensional character of the spin dynamics. The interchain exchange interaction which is responsible for three-dimensional correlations can be caused by the small S . . . S distances (compare Table I) between neighboring Cu-DTH complexes. The condensation into the nonmagnetic  $S=0$  ground state finally leads to the decrease of  $\Delta B_{1/2}$  for temperatures below  $\sim 20$  K.

### V. MAGNETIC SUSCEPTIBILITY

The static magnetic susceptibility of Cu-DTH was characterized by Hatfield *et al.*<sup>30</sup> From an analysis for temperatures below 26 K they determined the parameters  $J/k_B = -28.8$  K and  $\alpha = 0.87$ . The susceptibility was fitted by a formula which approximates the results of numerical calculations of finite systems with up to 10 sites.<sup>45</sup>

Johnston *et al.*<sup>9</sup> calculated the static susceptibility of the alternating Heisenberg spin 1/2 chain with high precision and published a formula which enables the accurate analysis of

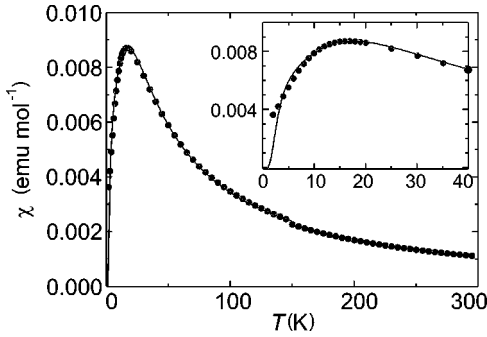


FIG. 10. Susceptibility of a polycrystalline sample of Cu-DTH (dots). The solid lines are calculated with the parameters  $J/k_B = -28.8$  K,  $\alpha = 0.87$ ,  $\bar{g} = 2.08$ , and  $\chi_0 = -7 \times 10^{-5}$  emu/mol. The inset shows the low-temperature range.

experimental results in the temperature range down to  $Tk_B/|J| = 0.01$ . In a recent paper Johnston, *et al.*<sup>15</sup> showed that it is even possible to disentangle the properties of two magnetically different alternating spin chains in  $(\text{VO})_2\text{P}_2\text{O}_7$ . Their fit formula<sup>46</sup> is therefore used for an analysis of the magnetic susceptibility of Cu-DTH below the structural phase transition. Figure 10 shows the static susceptibility of a polycrystalline sample of Cu-DTH (sample mass 19.951 mg) measured with a superconducting quantum interference device magnetometer (Quantum Design, Magnetic Property Measurement System) for a magnetic-field strength of 1 kOe in the temperature range 1.8–300 K. A small step at 150 K indicates the structural phase transition.

The solid line in Fig. 10 shows the expected temperature variation

$$\chi = \frac{(\bar{g}\mu_B)^2}{|J|} \chi^*(\alpha, t) + \chi_0 \quad (2)$$

with the parameters  $J/k_B = -28.8$  K and  $\alpha = 0.87$  of Hatfield *et al.*<sup>30</sup> and the average  $g$  factor of  $\bar{g} = 2.08$  of our ESR results.  $\chi^*(\alpha, t)$  denotes the formula of Johnston *et al.*<sup>46</sup> with  $t = k_B T/|J|$ . The temperature-independent susceptibility  $\chi_0 = -7(1) \times 10^{-5}$  emu/mol is fitted in the temperature range just below  $T_c$ .<sup>47</sup> The maximum of the susceptibility is well reproduced but not the low-temperature variation. The fit cannot be improved by simply adding the contribution of Curie-like defect spins. According to the structure of Cu-DTH below  $T_c$  there are two different chains. The results of Johnston *et al.*<sup>46</sup> enable the analysis of the susceptibility below the maximum. The fit parameters are  $J_1$ ,  $\alpha_1$ , and  $J_2$ ,  $\alpha_2$  of chain 1 and 2 ( $\bar{g}$  and  $\chi_0$  were not varied). The fit also includes the contribution of defect or impurity spins which are approximated by the Curie-law  $\chi_{\text{curie}} = C/T$ . Figure 11 shows the fitting results which lead to the parameters  $J_1/k_B = -29.3(1)$  K,  $\alpha_1 = 0.76(1)$  and  $J_2/k_B = -27.9(1)$  K,  $\alpha_2 = 0.99(1)$ ,  $C = 5.2(8) \times 10^{-4}$  emuK/mol. The rms deviation is  $\sigma_{\text{rms}} = 0.966\%$ .

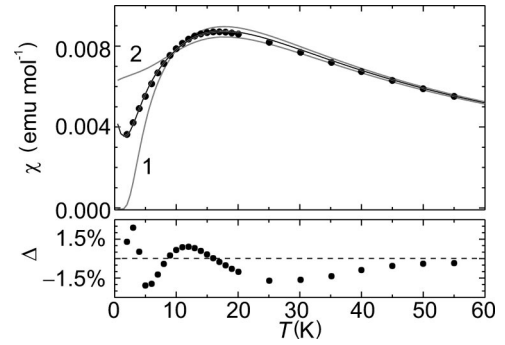


FIG. 11. Fit (solid line) of the susceptibility of Cu-DTH (dots) with two alternating spin chains (the parameters are given in the text). The lower panel shows the difference between the experiment and the fit  $\Delta = (\chi_{\text{exp}} - \chi_{\text{fit}})/\chi_{\text{exp}}$ . Curve 1 and 2 displays the susceptibility of chain 1 and 2, respectively.

The exchange and alternation parameters of the two chains correlate with the structural properties (Table I). The exchange  $J_1$  of chain 1 is stronger than  $J_2$  of chain 2 as can be expected from the shorter intradimer distance of chain 1. The smaller alternation parameter  $\alpha$  of chain 1 results from the larger interdimer distance of chain 1.

## VI. SUMMARY

We analyzed the crystallographic structure of Cu-DTH by x-ray diffraction below the structural phase transition. Cu-DTH forms a twin-domain structure and each domain consists of two inequivalent spin chains which are characterized by the exchange constants and alternation parameters  $J_1/k_B = -29.3(1)$  K,  $\alpha_1 = 0.76(1)$  and  $J_2/k_B = -27.9(1)$  K,  $\alpha_2 = 0.99(1)$ , respectively.

Above 150 K the ESR signal is characterized by one Lorentzian line. A temperature-dependent shift indicates the gradual development of Cu-DTH towards the phase transition. At the phase transition there is a hysteretic discontinuity and the ESR signal splits for special orientations of the magnetic field into two lines which is consistent with the formation of the twin-domain structure.

The magnitude and anisotropy of the linewidth are remarkably influenced by the phase transition. The analysis shows that the linewidth is dominated by the pseudodipolar exchange interaction and it turns out that the principal axes of the exchange tensor differ from those of the  $g$  tensor.

Although the static magnetic susceptibility is well characterized by a purely one-dimensional model the ESR signal indicates no one-dimensional spindynamics.

## ACKNOWLEDGMENTS

We thank Professor E. Dormann for helpful discussions. This work was supported by the Deutsche Forschungsgemeinschaft within the scope of the projects Nos. PI336/1-1,2 and PI336/3-1.

- <sup>1</sup>P.L. Nordio, Z.G. Soos, and H.M. McConnell, *Annu. Rev. Phys. Chem.* **17**, 237 (1966). *Chem.* **17**, 237 (1966).
- <sup>2</sup>U. Geiser, R.D. Willett, M. Lindbeck, and K. Emerson, *J. Am. Chem. Soc.* **108**, 1173 (1986).
- <sup>3</sup>C.P. Landee in *Organic and Inorganic Low-Dimensional Crystalline Materials*, Vol. 168 of *NATO Advanced Studies Institute, Series B: Physics*, edited by P. Delhaes and M. Drillon (Plenum, New York, 1987), pp. 75-92.
- <sup>4</sup>R.M. Lynden-Bell and H.M. McConnell, *J. Chem. Phys.* **37**, 794 (1962).
- <sup>5</sup>Bulaevskii, *Sov. Phys. JETP* **17**, 684 (1963).
- <sup>6</sup>A. Brooks Harris, *Phys. Rev. B* **7**, 3166 (1973).
- <sup>7</sup>M.C. Cross and D.S. Fisher, *Phys. Rev. B* **19**, 402 (1979).
- <sup>8</sup>I. Affleck, D. Gepner, H.J. Schulz, and T. Ziman, *J. Phys. A* **22**, 511 (1989).
- <sup>9</sup>D.C. Johnston, R.K. Kremer, M. Troyer, X. Wang, A. Klümper, S.L. Bud'ko, A.F. Panchula, and P.C. Canfield, *Phys. Rev. B* **61**, 9558 (2000).
- <sup>10</sup>I. Affleck, in *Field, Strings and Critical Phenomena*, Proceedings of the Les Houches Summer School, Session XLIX, edited by E. Brézin and J. Zinn-Justin (North-Holland, Amsterdam, 1990), pp. 565-640.
- <sup>11</sup>G. Chaboussant, M.-H. Julien, Y. Fagot-Revurat, M. Hanson, L.P. Lévy, C. Berthier, M. Horvatic, and M.O. Piovesana, *Eur. Phys. J. B* **6**, 167 (1998).
- <sup>12</sup>E. Dagotto, *Rep. Prog. Phys.* **62**, 1525 (1999).
- <sup>13</sup>T. Barnes and J. Riera, *Phys. Rev. B* **50**, 6817 (1994).
- <sup>14</sup>A.W. Garrett, S.E. Nagler, D.A. Tennant, B.C. Sales, and T. Barnes, *Phys. Rev. Lett.* **79**, 745 (1997).
- <sup>15</sup>D.C. Johnston, T. Saito, M. Azuma, M. Takano, T. Yamauchi, and Y. Ueda, *Phys. Rev. B* **64**, 134403 (2001).
- <sup>16</sup>J.C. Bonner and M.E. Fisher, *Phys. Rev.* **135**, A640 (1964).
- <sup>17</sup>W. Duffy and K.P. Barr, *Phys. Rev.* **165**, 647 (1968).
- <sup>18</sup>J.C. Bonner and H.W.J. Blöte, *Phys. Rev. B* **25**, 6959 (1982).
- <sup>19</sup>Z.G. Soos, S. Kuwajima, and J.E. Mihalick, *Phys. Rev. B* **32**, 3124 (1985).
- <sup>20</sup>D. Augier, D. Poilblanc, S. Haas, A. Delia, and E. Dagotto, *Phys. Rev. B* **56**, R5732 (1997).
- <sup>21</sup>T. Barnes, J. Riera, and D.A. Tennant, *Phys. Rev. B* **59**, 11 384 (1999).
- <sup>22</sup>M.J. Konstantinovic, K. Ladavac, A. Belic, Z.V. Popovic, A.N. Vasil'ev, M. Isobe, and Y. Ueda, *J. Phys.: Condens. Matter* **11**, 2103 (1999).
- <sup>23</sup>K.M. Diederix, H.W.J. Blöte, J.P. Groen, T.O. Klaassen, and N.J. Poulis, *Phys. Rev. B* **19**, 420 (1979).
- <sup>24</sup>J.C. Bonner, S.A. Friedberg, H. Kobayashi, D.L. Meier, and H.W.J. Blöte, *Phys. Rev. B* **27**, 248 (1983).
- <sup>25</sup>K.M. Diederix, J.P. Groen, L.S.J.M. Hengens, T.O. Klaassen, and N.J. Poulis, *Physica B* **93**, 99 (1978).
- <sup>26</sup>K.M. Diederix, J.P. Groen, L.S.J.M. Hengens, T.O. Klaassen, and N.J. Poulis, *Physica B* **94**, 9 (1978).
- <sup>27</sup>K.M. Diederix, J.P. Groen, T.O. Klaassen, and N.J. Poulis, *Phys. Rev. Lett.* **41**, 1520 (1978).
- <sup>28</sup>K.M. Diederix, J.P. Groen, T.O. Klaassen, and N.J. Poulis, *Physica B* **96**, 41 (1979).
- <sup>29</sup>G. Xu, C. Broholm, D.H. Reich, and M.A. Adams, *Phys. Rev. Lett.* **84**, 4465 (2000).
- <sup>30</sup>W.E. Hatfield, L.W. ter Haar, M.M. Olmstead, and W.K. Musker, *Inorg. Chem.* **25**, 558 (1986).
- <sup>31</sup>H. Henke, *Z. Kristallogr.* **178**, 91 (1987).
- <sup>32</sup>G. Sheldrick, computer code SHELX-97, a program for crystal structure refinement (Universität Göttingen, Göttingen, 1997).
- <sup>33</sup>H. Wondratschek, in *International Tables for Crystallography* (Reidel, Dordrecht, 1983), Vol. A.
- <sup>34</sup>With all torsional angles changing sign for instance.
- <sup>35</sup>J.B. Hendrickson, *J. Am. Chem. Soc.* **83**, 4537 (1961); **85**, 4059 (1963).
- <sup>36</sup>M.M. Olmstead, W.K. Musker, L.W. Ter Haar, and W.E. Hatfield, *J. Am. Chem. Soc.* **104**, 6627 (1982).
- <sup>37</sup>A. Abragam and B. Bleaney, *Electron Paramagnetic Resonance of Transition Ions* (Clarendon Press, Oxford, 1970).
- <sup>38</sup>T. Moriya, *Phys. Rev.* **120**, 91 (1960).
- <sup>39</sup>J. Kanamori in *Magnetism*, edited by G.T. Rado and H. Suhl (Academic Press, New York, 1963), Vol. 1, p. 127.
- <sup>40</sup>L. Banci, A. Bencini, and D. Gatteschi, *J. Am. Chem. Soc.* **105**, 761 (1983).
- <sup>41</sup>B. Pilawa, E. Herrling, and I. Odenwald, *J. Magn. Magn. Mater.* **226-230**, 417 (2001).
- <sup>42</sup>the secular component of the anisotropic interaction commutes with the total spin  $S^z$ .
- <sup>43</sup>D.W. Hone and P.M. Richards, *Annu. Rev. Mater. Sci.* **4**, 337 (1974).
- <sup>44</sup>G.F. Reiter and J.P. Boucher, *Phys. Rev. B* **11**, 1823 (1975).
- <sup>45</sup>J.W. Hall, W.E. Marsh, R.R. Weller, and W.E. Hatfield, *Inorg. Chem.* **20**, 1033 (1981).
- <sup>46</sup>Formula (56a) in Ref. 9.
- <sup>47</sup>This value is in the range of the expected diamagnetic susceptibility of Cu-DTH.  $\chi_0(\text{Cu-DTH}) \approx -14.7 \times 10^{-5}$  emu/mol can be estimated with the diamagnetic susceptibility of  $\text{Cu}^{\text{II}}$  ( $-1.1 \times 10^{-5}$  emu/mol),  $\text{Cl}^-$  ( $-2.6 \times 10^{-5}$  emu/mol) and  $\text{C}_6\text{H}_{14}\text{S}_2$  ( $-8.4 \times 10^{-5}$  emu/mol), see *Magnetic Properties of Transition Metal Compounds*, edited by K. H. Hellwege and A. M. Hellwege, Landolt Börnstein, New Series, Group II, Vol. 10 (Springer-Verlag, Berlin, 1967).
- <sup>48</sup>See EPAPS Document No. E-PRBMDO-67-019301 for structural data of the low-temperature phase of dichloro(2,5-dithiahexane) copper(II). A direct link to this document may be found in the online article's HTML reference section. The document may also be reached via the EPAPS homepage (<http://www.aip.org/pubservs/epaps.html>) or from [ftp.aip.org](ftp://ftp.aip.org) in the directory /epaps/. See the EPAPS homepage for more information.